

# Small-scale properties of Class 0 protostars from the CALYPSO IRAM-PdBI survey

Anaëlle Maury<sup>1</sup>, Philippe André<sup>1</sup>, Sébastien Maret<sup>2</sup>,  
Arnaud Belloche<sup>3</sup>, Claudio Codella<sup>4</sup>, Sylvie Cabrit<sup>2</sup>, Frédéric Gueth<sup>5</sup>  
and CALYPSO collaboration<sup>1</sup>

<sup>1</sup>Laboratoire AIM, CEA/DSM-CNRS-Université Paris Diderot, France

email: [anaelle.maury@cea.fr](mailto:anaelle.maury@cea.fr)

<sup>2</sup>IPAG, Grenoble, France

<sup>3</sup>MPIfR Bonn, Germany

<sup>4</sup>INAF, Osservatorio Astrofisico di Arcetri, Firenze, Italy

<sup>5</sup>IRAM, Grenoble, France

**Abstract.** Because the formation of protostars is believed to be closely tied to the angular momentum problem of star formation, characterizing the properties of the youngest disks around Class 0 objects is crucial. However, not much is known on the structure of the youngest protostellar envelopes, on the small scales at which disks and multiple systems are observed around more evolved YSOs, due to a lack of comprehensive high angular resolution observations (probing  $<100$  AU). In order to tackle this issue, we conducted a large observing program with the IRAM Plateau de Bure interferometer (PdBI): the CALYPSO survey, providing us with detailed maps of molecular lines and millimeter continuum emission, probing scales down to  $\sim 30$ – $50$  au towards a sample of 17 Class 0 protostars. Here we present our analysis of the CALYPSO dust continuum emission maps, constraining disk properties of the Class 0 protostars in our sample. We show that large,  $r > 50$  au, disk structures are not observed in most Class 0 protostars from our sample, which can be described by various envelope models reproducing satisfactorily the intensity distribution of the dust emission at all scales from 50 au to 5000 au.

**Keywords.** Class 0 Protostars, Circumstellar Disks, IRAM-PdBI, CALYPSO

---

## 1. Introduction

Young Class 0 protostars (André *et al.* 2000), observed only  $t \lesssim 5 \times 10^4$  yr after their formation, still have most of their mass in the form of a dense core/envelope collapsing onto the central protostellar embryo: they are representative of the main accretion phase, during which most of the final stellar mass is accreted onto the central object. During this protostellar phase, the inflowing gas must redistribute most of its initial angular momentum outward or else centrifugal forces will balance gravity and prevent accretion, and the growth of the protostellar embryo. This long-standing “angular momentum problem” is quite severe since the gas must reduce its specific angular momentum by  $\sim 5$  orders of magnitude during this brief accretion phase ( $<0.1$  Myr) (Belloche 2013). Exactly how this is done remains a major unsolved problem in star formation. Early theoretical studies (Terebey *et al.* 1984) suggested that the formation of large ( $\geq 100$  au) centrifugally supported disks and protostellar jets (Shu *et al.* 1991) would transfer angular momentum outward, contributing grandly to solving the angular momentum problem by the end of the first collapse phase. However, while the presence of large (radii 100–300 au) accretion disks is well documented in Class I protostars and T-Tauri stars (Watson *et al.* 2007; Duchêne *et al.* 2007; Connelley *et al.* 2008), the progenitors of these protoplanetary disks remain elusive around younger Class 0 protostars (Maury *et al.* 2010; Ohashi *et al.* 2014;

Yen *et al.* 2015a). Whether disks and multiple systems are natural products of the conservation of angular momentum formed during the main accretion phase remains largely debated today from both an observational and a theoretical point of view.

## 2. The CALYPSO survey

The CALYPSO survey (see <http://irfu.cea.fr/Projets/Calypso/>), carried out with the IRAM Plateau de Bure (PdBI) interferometer, has been tailored to address this cornerstone question, and ultimately describe how the circumstellar envelope is being accreted onto the central protostellar embryo, also exploring the formation processes of protostellar jets, disks and multiple systems, during the main accretion phase. In the framework of this IRAM large program, we carried out detailed dust continuum and molecular line emission observations of 17 Class 0 protostars, at scales ranging from 50 au to 5000 au, in selected frequency ranges between 1.3 mm and 3.2 mm. Highlights of the CALYPSO observations of the Class 0 protostar NGC1333-IRAS2A (IRAS2A in the following) were presented in Maret *et al.* (2014), Maury *et al.* (2014) and Codella *et al.* (2014).

## 3. Analysis of the dust continuum emission

Here we briefly present our analysis of the dust continuum emission obtained in the 1mm PdBI bands, namely two independent observations obtained over 4-GHz bandwidths centered respectively at 1.3 mm and 1.4 mm, towards a large fraction of the CALYPSO sample, analyzed as of August 2015 and presented in Table 1.

Class 0 protostars are heavily embedded, envelope-dominated sources. To constrain the protostellar disk properties during this early stage, a precise modeling of envelope emission at all scales is required to discriminate envelope emission from disk emission at small scales. The large-scale envelope structure is recovered thanks to IRAM-30m 1.2-mm continuum observations used as zero-spacing information as well as short-spacing intensity profiles when available (see Motte & André 2001). The IRAM-30m 1.2-mm dust continuum emission maps (Motte & André 2001) tracing protostellar envelopes at large scales  $\sim 10 - 50''$  are shown in the left panels of Figs. 1, 2 and 3, while the central panels show the IRAM-PdBI 1.3-mm dust continuum maps, sensitive to the inner envelope density structure at scales  $\sim 0.5 - 5''$ . We examine the flux density versus uv-distance from the PdBI data at both 1.3 mm and 1.4 mm, and use Plummer-like envelope models with  $\rho(r) = \rho_0 \left( \frac{R_0}{\sqrt{r^2 + R_0^2}} \right)^p$  to reproduce the visibility profiles observed at the two wavelengths (see central panels of Figs. 1, 2 and 3). In the Rayleigh-Jeans approximation and for optically-thin dust emission, if the temperature and density in the envelope follow simple radial power laws  $\rho(r) \propto r^{-p}$  and  $T(r) \propto r^{-q}$ , the emergent dust continuum emission also has a simple power-law form  $I(r) \propto r^{-p-q+1}$ . In interferometric observations, the visibility distribution then has  $V(b) \propto b^{p+q-3}$ , solely determined by the power-law indices of the temperature and density profiles in the envelope. We noticed that the PdBI 1.3 mm visibility curves were not satisfactorily reproduced by envelope models, for a few sources in our sample. To check whether this deviation to a single envelope profile traces a circumstellar disk embedded in the envelope, or reflects envelope asymmetries and structure, we also tried to reproduce the intensity profiles with models including the best-fit envelope model and a Gaussian source of variable flux and size, tracing a candidate disk structure. The details of this analysis will be presented in a forthcoming paper (Maury *et al.* in prep.). It is illustrated for three of our CALYPSO sources in Figs. 1 to 3. The right panels show the visibilities fluxes as a function of IRAM-PdBI baseline length. The best-fit Plummer envelope model reproducing the single dish continuum emission profile (at baselines  $< 20$  k $\lambda$ , e.g. tracing the outer envelope properties) is shown as a red curve, for each source. The main results of our analysis, such as best-fit values of the

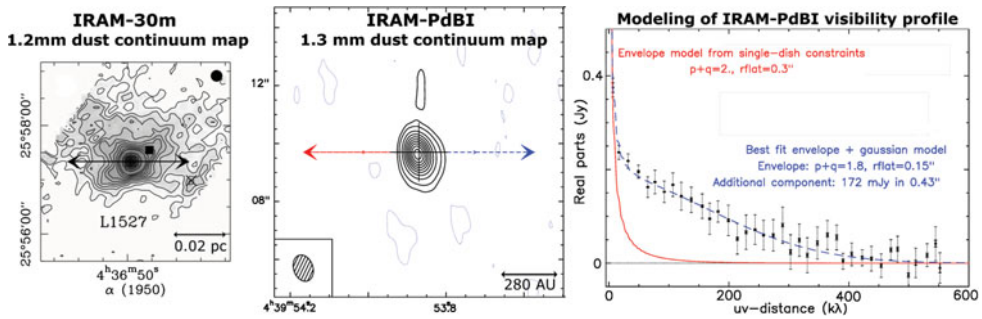


**Figure 1.** L1527: Dust continuum emission from the IRAM-30 m (map shown in left panel) and PdBI (map shown in central panel, the double-sided arrow marks the outflow axis) is reproduced with a model featuring a Plummer envelope and an additional Gaussian source. The best-fitting model includes a  $r \sim 60$  au radius additional Gaussian source at phase center, interpreted as a candidate disk component, and is shown in the right panel as a blue curve overlaid on the PdBI visibility profile at 1.3 mm. (*A color version of this figure is available online.*)

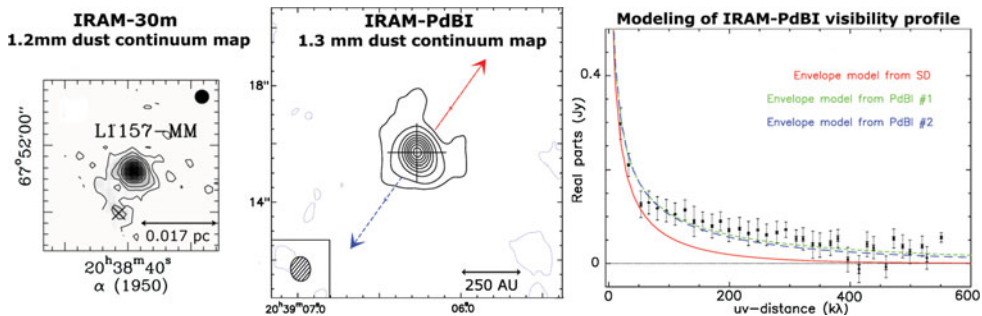


**Figure 2.** L1157: Dust continuum emission from the IRAM-30 m (map shown in left panel) and PdBI (map shown in central panel, the double-sided arrow marks the outflow axis) is well reproduced with a model only comprising a Plummer envelope. The best model is shown as a blue curve in the right panel: it does not need any additional Gaussian component to reproduce the PdBI 1.3-mm visibility profile apart from the envelope model, therefore suggesting any protostellar disk is  $r < 40$  au in this Class 0 source. (*Color version available online.*)

power-law indices for protostellar envelopes and detection of a  $r > 50$  au candidate-disk component, are summarized in Table 1.

#### 4. Summary: do most Class 0 protostellar disks have radii $< 50$ au ?

Among the 12 Class 0 protostars analyzed here, only 3 of them show millimeter dust continuum visibility profiles which may hint to the presence of disk structures with radii  $> 50$  au, and only one source may harbor a candidate disk with radius  $> 100$  au. Being the largest sample of Class 0 protostars analyzed so far, our results confirm the paucity of large Class 0 disks suggested by recent literature (Maury *et al.* 2010, Yen *et al.* 2015, Tobin *et al.* 2015). These upper limits on disk sizes are not easily explained by the standard hydrodynamical description of protostellar collapse, where large ( $r > 100$  au) disk-like structures are expected to form quickly ( $t < 10^3$  yr) at the beginning of the protostellar phase, as a consequence of angular momentum conservation during collapse of the large-scale envelope towards the central protostellar embryo (Li *et al.* 2014). One possible explanation for the regulation of disk sizes during the main accretion phase, lies in magnetically-regulated protostellar collapse scenarios, because magnetic braking can significantly contribute to angular momentum transport and hence delay the formation of large disk-structures (Hennebelle & Teyssier 2008). In the sources showing no signs of

**Table 1.** Preliminary results from the analysis of continuum emission in the CALYPSO sample

Object	$\alpha$ (J2000)	$\delta$ (J2000)	Dist. (pc)	$M_{env}$ ( $M_{\odot}$ ) (1)	$F_{peak}^{PdBI} / F_{tot}^{SD}$ (2)	$p + q$ index (3)	Candidate > 50 au disk ? (4)	Class
L1448-2A	03:25:22.406	+30:45:13.28	220	0.9	0.09-0.10	2-2.3	n	0
L1448-NB	03:25:36.364	+30:45:14.83	220	1	0.1-0.13	2.6-2.8	n	0
L1448-C	03:25:38.878	+30:44:05.32	220	4	0.14-0.18	2.3-2.6	n	0
IRAS2A	03:28:55.575	+31:14:37.05	220	5	0.15-0.2	2.5-2.6	n	0
SVS13-B	03:29:03.075	+31:15:51.71	220	3	0.15-0.2	1.7-2.1	y	0
IRAS4A	03:29:10.531	+31:13:30.96	220	6	0.4-0.6	2.7-2.8	n	0/I
IRAS4B	03:29:12.012	+31:13:08.07	220	3	0.2-0.3	2.7-2.9	y	0
IRAM04191	04:21:56.903	+15:29:46.14	140	1	0.006	1.5-1.6	n	0
L1521-F	04:28:38.936	+26:51:35.11	140	0.7	0.01-0.04	1.4-1.7	n	0
L1527	04:39:53.874	+26:03:09.67	140	1	0.13-0.15	1.8-2.0	y	0/I
L1157	20:39:06.268	+68:02:15.67	250	1.5	0.11-0.13	2.5-2.6	n	0
GF9-2	20:51:30.29.822	+60:18:38.44	200	0.5	<0.04	1.7-1.9	n	0

(1) Envelope masses from the literature. (2) Ratio of the small-scale flux (1.3-mm peak flux computed in PdBI matching-beams maps – synthesized HPBW  $\sim 1.5'' \times 1''$ ) to the total envelope flux (as extrapolated from IRAM-30m 1.2-mm or Bolocam 1.1-mm dust continuum maps). (3) Index of the intensity profile, see Maury *et al.* (2014). (4) Indicating whether the best model to reproduce both the IRAM-30m and IRAM-PdBI continuum emission includes a Gaussian source of FWHM > 50 au (“y” for yes or “n” for no).

large disks, the role of magnetic fields should be explored in more detail to understand our puzzling results. The kinematics of Class 0 envelopes will have to be explored as well, for example to look for signatures of transitions to Keplerian rotation at small scales in the sources where additional dust continuum structures are needed to explain our PdBI data: the wealth of density and temperature regimes probed by the CALYPSO molecular line observations should allow such investigations in the coming year.

## Acknowledgements

This work has received support from the ERC ‘ORISTARS’ project (ERC Advanced Grant Agreement no. 291294).

## References

- André, P., Ward-Thompson, D., & Barsony, M., 2000, in *Protostars and Planets IV*, p. 59
- Belloche, A., 2013, in *EAS Publications Series* Vol. 62, pp 25
- Codella, C., Maury, A. J., Gueth, F., *et al.*, 2014, *A&A*, 563, L3
- Connelley, M. S., Reipurth, B., & Tokunaga, A. T. 2008, *ApJ*, 135, 2526
- Duchêne, G., Bontemps, S., Bouvier, J., *et al.*, 2007, *A&A*, 476, 229
- Hennebelle, P. & Teyssier, R., 2008, *A&A*, 477, 9
- Li Z.-Y., *et al.*, 2014, *Protostars and Planets VI*, pp 173
- Maret, S., Belloche, A., Maury, A. J., *et al.*, 2014, *A&A*, 563, L1
- Maury, A. J., André, Ph. *et al.*, 2010, *A&A*, 512, A40+
- Maury, A. J., Belloche, A., André, Ph. *et al.*, 2014, *A&A*, 563, L2
- Maury, A. J., *et al.*, 2016, in prep., *A&A*
- Motte, F. & André, Ph., 2001, *A&A*, 365, 440
- Ohashi, N., Saigo, K., Aso, Y., *et al.* 2014, *ApJ*, 796, 131
- Terebey, S., Shu, F., & Cassen, P., 1984, *ApJ*, 286, 529
- Tobin, J., *et al.* 2015, *ApJ*, 805, 125
- Shu, F. H., Ruden, S. P., Lada, C. J., & Lizano, S., 1991, *ApJ*, 370, 31
- Watson, A. M., Stapelfeldt, K. R., *et al.*, 2007, in *Protostars and Planets V*, p. 523
- Yen, H.-W., Koch, P. M., Takakuwa, S., *et al.* 2015, *ApJ*, 799, 193
- Yen, H.-W., Takakuwa, S., Koch, P. M., *et al.* 2015, *ApJ*, 812, 129